Anal. Chem. **2005,** *77,* 1539−1544

Accelerated Articles

Selective Encapsulation of Single Cells and Subcellular Organelles into Picoliter- and Femtoliter-Volume Droplets

Mingyan He, J. Scott Edgar, Gavin D. M. Jeffries, Robert M. Lorenz, J. Patrick Shelby, and Daniel T. Chiu*

Department of Chemistry, University of Washington, Seattle, Washington 98195-1700

This paper describes a method, which combines optical trapping and microfluidic-based droplet generation, for selectively and controllably encapsulating a single target cell or subcellular structure, such as a mitochondrion, into a picoliter- or femtoliter-volume aqueous droplet that is surrounded by an immiscible phase. Once the selected cell or organelle is encased within the droplet, it is stably confined in the droplet and cannot be removed. We demonstrate in droplet the rapid laser photolysis of the single cell, which essentially "freezes" the state that the cell was in at the moment of photolysis and confines the lysate within the small volume of the droplet. Using fluorescein di-β-D-galactopyranoside, which is a fluorogenic substrate for the intracellular enzyme β-galactosidase, we also assayed the activity of this enzyme from a single cell following the laser-induced lysis of the cell. This ability to entrap individual selected cells or subcellular organelles should open new possibilities for carrying out single-cell studies and single-organelle measurements.

We are exploring the use of aqueous droplets that range in volume from a few picoliters to subfemtoliters as reaction vessels for the chemical manipulation of single cells, individual subcellular organelles, and single molecules.[1,2] Aqueous droplets represent an important area of research in downscaled analytical techniques[3−5] as reflected in the wide range of work in the literature on levitating droplets in air[5−9] and in detecting molecules within such droplets.[8,9] Aqueous droplets with monodisperse size can be generated in microfluidic systems,[10−16] the analytes contained within droplets can be highly concentrated,[2] and individual aqueous droplets can be fused[1,17−19] and transported.[18−22] Although these droplet manipulations have been demonstrated separately using a wide range of approaches, much work still remains in integrating these different manipulations into a single platform. For example, the degree of control required in the formation of a single subpicoliter-

* To whom correspondence should be addressed. E-mail: chiu@chem.washington.edu.

(1) Chiu, D. T. *TrAC−Trends Anal. Chem.* **2003**, *22*, 528−536.
(2) He, M. Y.; Sun, C. H.; Chiu, D. T. *Anal. Chem.* **2004**, *76*, 1222−1227.
(3) Yi, C.; Huang, D. J.; Gratzl, M. *Anal. Chem.* **1996**, *68*, 1580−1584.
(4) Suwa, M.; Watarai, H. *Anal. Chem.* **2001**, *73*, 5214−5219.
(5) Petersson, M.; Nilsson, J.; Wallman, L.; Laurell, T.; Johansson, J.; Nilsson, S. *J. Chromatogr., B* **1998**, *714*, 39−46.
(6) Omrane, A.; Santesson, S.; Alden, M.; Nilsson, S. *Lab Chip* **2004**, *4*, 287−291.
(7) Welter, E.; Neidhart, B. *Fresenius J. Anal. Chem.* **1997**, *357*, 345−350.
(8) Santesson, S.; Andersson, M.; Degerman, E.; Johansson, T.; Nilsson, J.; Nilsson, S. *Anal. Chem.* **2000**, *72*, 3412−3418.
(9) Barnes, M. D.; Ng, K. C.; Whitten, W. B.; Ramsey, J. M. *Anal. Chem.* **1993**, *65*, 2360−2365.
(10) Thorsen, T.; Roberts, R. W.; Arnold, F. H.; Quake, S. R. *Phys. Rev. Lett.* **2001**, *86*, 4163−4166.
(11) Liu, H. J.; Nakajima, M.; Kimura, T. *J. Am. Oil Chem. Soc.* **2004**, *81*, 705−711.
(12) Tan, Y. C.; Fisher, J. S.; Lee, A. I.; Cristini, V.; Lee, A. P. *Lab Chip* **2004**, *4*, 292−298.
(13) Tice, J. D.; Song, H.; Lyon, A. D.; Ismagilov, R. F. *Langmuir* **2003**, *19*, 9127−9133.
(14) Song, H.; Tice, J. D.; Ismagilov, R. F. *Angew. Chem., Int. Ed.* **2003**, *42*, 768−772.
(15) Kawakatsu, T.; Tragardh, G.; Tragardh, C.; Nakajima, M.; Oda, N.; Yonemoto, T. *Colloid Surf. A* **2001**, *179*, 29−37.
(16) Anna, S. L.; Bontoux, N.; Stone, H. A. *Appl. Phys. Lett.* **2003**, *82*, 364−366.
(17) Yao, H.; Ikeda, H.; Inoue, Y.; Kitamura, N. *Anal. Chem.* **1996**, *68*, 4304−4307.
(18) Pollack, M. G.; Shenderov, A. D.; Fair, R. B. *Lab Chip* **2002**, *2*, 96−101.
(19) Cho, S. K.; Moon, H. J.; Kim, C. J. *J. Microelectromech. Syst.* **2003**, *12*, 70−80.
(20) Kuo, J. S.; Spicar-Mihalic, P.; Rodriguez, I.; Chiu, D. T. *Langmuir* **2003**, *19*, 250−255.
(21) Chiou, P. Y.; Moon, H.; Toshiyoshi, H.; Kim, C. J.; Wu, M. C. *Sens. Actuators, A* **2003**, *104*, 222−228.
(22) Chaudhury, M. K.; Whitesides, G. M. *Science* **1992**, *256*, 1539−1541.

10.1021/ac0480850 CCC: $30.25
Published on Web 02/12/2005

or femtoliter-volume aqueous droplet followed by its transport and fusion to another single droplet generated on demand has yet to be developed. Most of the work performed thus far involves large aqueous droplets that range in size from a few tens to hundreds of picoliters for those immersed in oil[11−14,16] and microliters to nanoliters for those in contact with air.[7,8,18,19,21,22] The generation and manipulation of a single femtoliter-volume aqueous droplet in microfluidic channels also pose significant technical challenges.

Toward developing a platform that uses individual pico- and femtoliter-volume aqueous droplets as reaction containers for single-cell and single-organelle measurements, this paper demonstrates for the first time the ability to selectively introduce a single cell or organelle into an aqueous droplet in microfluidic channels. Once encapsulated within the droplet, the cell or organelle can be stably confined and assays can be performed. In comparison with open volumes, the confined volume defined by the droplet prevents dilution of the molecules of interest. In addition, the concentration of the molecules within the droplet can be drastically increased without heating the droplet,[2] a characteristic that is especially useful in reacting molecules (e.g., signaling proteins) that are present in low copy numbers. Here following selective encapsulation of single cells and mitochondria within droplets, we also demonstrate in droplets the rapid photolysis of single cells and the assay of enzymatic activity of a single cell. Although this paper focuses on aqueous droplets, we believe our method can be applied equally well to the formation and manipulation of organic droplets, which represent an active area of research.[23−33]

EXPERIMENTAL SECTION

Fabrication of Microchannels. Silicon masters with patterned SU-8 negative photoresist were fabricated using photolithography as described in detail elsewhere.[34,35] For two-layer patterns with different thicknesses of SU-8, we used two-step photolithography. Here the thin (e.g., 10 μm) layer was fabricated and developed first, after which we spin coated onto this developed one-layer master a second thicker (e.g., 50 μm) layer of SU-8. The features on the first layer and the second layer were carefully aligned using alignment marks under a mask aligner. After alignment and exposure, the second layer was developed and the patterned master was silanized overnight with tridecafluoro-1,1,2,2-tetrahydrooctyl-1-trichlorosilane.

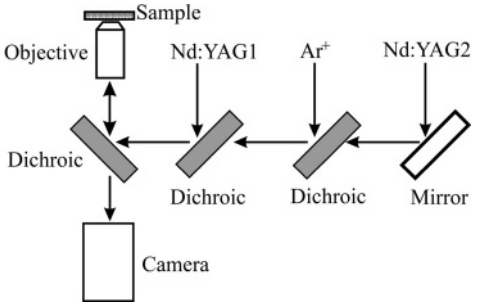

Figure 1. Simplified schematic of our optical setup. Nd:YAG1 is a frequency-tripled (355 nm) pulsed YAG laser with a ~5-ns pulse duration, which we used for the photolysis of single cells. The Ar^+ laser (at 488 nm) was used to excite fluorescence, and the Nd:YAG2 (continuous wave at 1064 nm) was used for optical trapping.

To form the microchannels, the pattern on the master was replicated in poly(dimethylsiloxane) (PDMS)[2,35−38] and then bonded to a coverslip with a thin layer of spin-coated PDMS. It was necessary to coat the coverslip with PDMS because the generation of aqueous droplets required channels with four hydrophobic walls to prevent wetting of the aqueous phase onto the walls of the channel. The layer of PDMS on our coverslip (Gold Seal with thickness of 130−160 μm and Corning with thickness of 160−190 μm) must be very thin (<10 μm) to be compatible with our high numerical aperture (NA) objectives (Nikon, 100×, NA 1.3, with a working distance of 200 μm) for optical trapping and laser photolysis. To spin coat this thin PDMS layer, we diluted the PDMS prepolymer solution in *n*-heptane at a weight ratio of 1:2 to decrease its viscosity. To ensure thorough curing, the coated PDMS layer was left in a 120 °C oven for at least 1 day.

To plumb the microchannels, access holes to the channels were made with a 16-gauge blunt needle. Polyethylene tubings (PE100) were inserted into the access holes and then attached to 1-mL syringes through which fluids were introduced into the channels. A syringe pump (Braintree Scientific, Braintree, MA) was used to deliver oil into channels, while the aqueous phase was delivered by manually pushing the syringe. For the immiscible phase, we used either silicone oil (AR 20, Fluka, Buchs, Switzerland) with 3% (w/w) sorbitan trioleate (Span 85, Fluka, Buchs, Switzerland) or soybean oil (Ventura Foods, City of Industry, CA) that had been degummed and saturated with deionized water. The silicone oil is polyphenyl−methylsiloxane with a density of 1.008 g/mL and viscosity of 20 mPa·s (25 °C). The soybean oil has a density of 0.927 g/mL and viscosity of 69 mPa·s (20 °C). We chose these two oils because they work well with PDMS and their densities are comparable to that of water. Although silicone oil slightly swells PDMS, the effect was negligible for our experiment.

Fluorescence Imaging, Optical Trapping, and Laser Photolysis. Figure 1 depicts our home-built optical setup. An Ar^+ laser (wavelength at 488 nm, Spectra-Physics Lasers, Mountain View, CA) was used to excite fluorescence, and a sensitive camera (Cohu 4910, San Diego, CA) was used for fluorescence imaging. Optical

(23) Monjushiro, H.; Tanaka, M.; Watarai, H. *Chem. Lett.* **2003**, *32*, 254−255.
(24) Suwa, M.; Watarai, H. *Anal. Chem.* **2002**, *74*, 5027−5032.
(25) Sakai, T.; Takeda, Y.; Mafune, F.; Kondow, T. *J. Phys. Chem. B* **2004**, *108*, 6359−6364.
(26) Sakai, T.; Takeda, Y.; Mafune, F.; Abe, M.; Kondow, T. *J. Phys. Chem. B* **2003**, *107*, 2921−2926.
(27) Sakai, T.; Takeda, Y.; Mafune, F.; Abe, M.; Kondow, T. *J. Phys. Chem. B* **2002**, *106*, 5017−5021.
(28) Sugiura, S.; Nakajima, M.; Seki, M. *Langmuir* **2002**, *18*, 5708−5712.
(29) Sugiura, S.; Nakajima, M.; Kumazawa, N.; Iwamoto, S.; Seki, M. *J. Phys. Chem. B* **2002**, *106*, 9405−9409.
(30) Sugiura, S.; Nakajima, M.; Seki, M. *Langmuir* **2002**, *18*, 3854−3859.
(31) Kogi, O.; Yuya, K.; Kim, H. B.; Kitamura, N. *Langmuir* **2001**, *17*, 7456−7458.
(32) Kogi, O.; Kim, H. B.; Kitamura, N. *Anal. Chim. Acta* **2000**, *418*, 129−135.
(33) Tong, J. H.; Nakajima, M.; Hiroshi; Nabetani; Kikuchi, Y. *J. Surfactants, Deterg.* **2001**, *4*, 85.
(34) Fiorini, G. S.; Lorenz, R. M.; Kuo, J. S.; Chiu, D. T. *Anal. Chem.* **2004**, *76*, 4697−4704.
(35) Anderson, J. R.; Chiu, D. T.; Jackman, R. J.; Cherniavskaya, O.; McDonald, J. C.; Wu, H. K.; Whitesides, S. H.; Whitesides, G. M. *Anal. Chem.* **2000**, *72*, 3158−3164.
(36) Allen, P. B.; Rodriguez, I.; Kuyper, C. L.; Lorenz, R. M.; Spicar-Mihalic, P.; Kuo, J. S.; Chiu, D. T. *Anal. Chem.* **2003**, *75*, 1578−1583.
(37) McDonald, J. C.; Duffy, D. C.; Anderson, J. R.; Chiu, D. T.; Wu, H. K.; Schueller, O. J. A.; Whitesides, G. M. *Electrophoresis* **2000**, *21*, 27−40.
(38) Xia, Y. N.; Whitesides, G. M. *Angew. Chem., Int. Ed.* **1998**, *37*, 551−575.

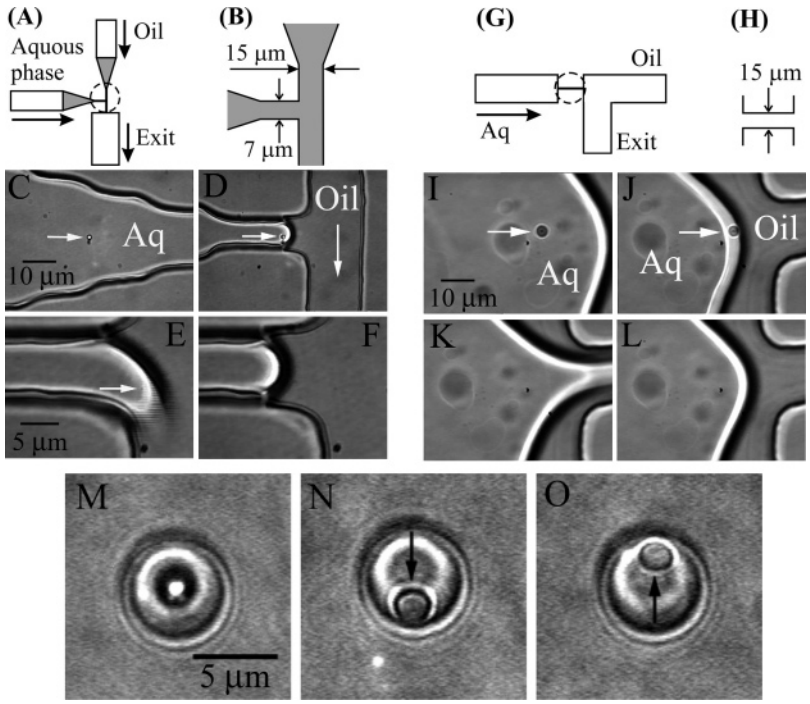

Figure 2. Schematics and sequences of images showing the two microfluidic designs we used for the encapsulation of single micro- and nanoparticles into droplets. (A, B) Schematic of a T channel, in which the aqueous droplet is sheared off at the junction by the flowing oil phase; the circled area in (A) is expanded in (B). Shaded areas in (A, B) are the shallow (10 μm) channels, and the rest are deep (50 μm) channels. (C−F) Images showing the optical trapping and transport of a selected bead to the T-junction (C, D). Once the bead was parked and maintained at the interface of the two fluids, a pressure pulse was applied to the aqueous phase to shear off a single droplet (E, F). The bead was entrapped within the droplet during this formation process and thus was removed from the T-junction (F). (G, H) Schematic of a second design we used for forming droplets, in which the aqueous phase is pushed through a channel constriction into an immiscible phase. (H) is the expanded drawing of the circled area in (G). To introduce a bead into the droplet, we again optically trapped and transported the bead to the interface (I, J) so that the bead was enclosed within the droplet as the droplet was being generated (K, L). Once a bead was encapsulated within the droplet (M), it can be freely moved within the droplet by optical trapping, but it cannot be forced across the interface and be removed from the droplet (N, O). The immiscible phase was soybean oil. Scale bars in (C) applies to (D), in (E) applies to (F), in (I) applies to (J−L), and in (M) applies to (N, O).

trapping was carried out by using a continuous-wave Nd:YAG laser (wavelength at 1064 nm, Spectra-Physics Lasers), while laser photolysis was performed with a ~5-ns pulsed frequency-tripled YAG laser (wavelength at 355 nm, Continum, Santa Clara, CA). The three laser beams were aligned collinearly and combined using dichroics, after which they were sent into a high-NA (1.3) objective of an inverted microscope (Nikon TE 300, Nikon, Tokyo, Japan). Fast imaging was achieved with a high-speed camera (CPL-MS4K, Canadian Photonic Labs, Minnedosa, Manitoba, Canada).

Preparation of Cells and Mitochondria. Mouse mast cells (ATCC, Manassas, VA) and B lymphocytes (ATCC, Manassas, VA) were grown in cell culture media and incubated at 37 °C and 5% CO_2. The culture medium was RPMI-1640 (Invitrogen, Carlsbad, CA) supplemented with 10% newborn calf serum (Invitrogen) and 1% penicillin−streptomycin solution (Sigma, St. Louis, MO).

To assay the activity of β galactosidase from single cells confined within droplets, we used the fluorogenic substrate fluorescein di-β-D-galactopyranoside (FDG, Molecular Probes, Eugene, OR). Right before the experiment, 20 μL of 50 mM FDG in dimethyl sulfoxide was mixed with 100 μL of mast cell suspension in culture media as our disperse phase. The time lag between the mixing of FDG with cell suspension and the actual enzymatic assay was ~20 min.

Mitochondria were isolated from mast cells using a commercially available Pierce Mitochondria Isolation Kit (Pierce Biotechnology, Inc, Rockford, IL). After centrifugation, the mitochondria pellet was suspended in a trypsin−EDTA isotonic solution (0.25% trypsin, Invitrogen). Mitochondria were labeled with 3 μM (final dye concentration) Mitotracker Green FM (Molecular Probes). The final labeled mitochondrial sample was kept on ice until used in the experiments.

RESULTS AND DISCUSSIONS

Controlled Encapsulation of an Optically Trapped Particle into a Single Femtoliter-Volume Aqueous Droplet. We used two methods to generate aqueous droplets and to encapsulate particles into the droplets. Both methods required microchannels with hydrophobic surfaces to prevent wetting of the aqueous phase to the channel walls. To encapsulate a select particle into a droplet, optical trapping was used to manipulate and translate the desired particle to the interface of the two immiscible fluids so that the particle would be enclosed within the droplet during the droplet formation process. Here the key requirement is the ability to generate controllably a single droplet having the desired size on demand after the particle had been positioned at the interface of the two fluids. Figure 2A,B and G,H depicts the two approaches we used to form droplets.

The first method is based on a T-channel design (Figure 2A,B).[10,13,14] Here the shear force exerted by the oil phase on the interface of the two fluids causes droplet formation. The size of a droplet generated with this method can be approximated by equating the Laplace pressure with the shear stress:[10,39,40]

$$R \approx \sigma/\eta\dot{\epsilon} \quad (1)$$

where R is the radius of the droplet, σ is the interfacial tension between aqueous and oil phases (e.g., interfacial tension between soybean oil and water is 22.8 mN/m[41]), η is the viscosity of the oil phase, and $\dot{\epsilon}$ is the shear rate. The shear rate is determined by the channel size and the velocity of the oil phase across the gap at the T-junction.[10] The shear rate we employed in our experiments was in the range of 10^4-10^5 s^{-1}, depending on the type of immiscible phase and surfactants we used and the size of the droplet we generated. In Figure 2C−F, for example, the shear rate was $\sim 1 \times 10^5$ s^{-1} and the shear stress was $\sim 8 \times 10^3$ Pa. Smaller channel size and higher velocity of the oil phase at the T-junction lead to the formation of droplets with smaller radii. The advantage of this method is the ease with which a continuous stream of droplets with a defined size can be formed. The use of this method to form a single droplet as needed in our experiments, however, requires special channel designs and precise pressure control.

We found single droplets can be formed more easily when the branches of the T-junction are short, which reduces pressure drop of both phases. A narrow T-branch for the aqueous phase helps to control the formation of a single droplet. Because the generation of a single droplet and the encapsulation of a bead into it requires stopping the flow of both the aqueous and the oil phases, it is also important to prevent the attachment of the beads and the droplets to the surface of the channel walls. Based on these considerations, we designed our T-junction to be very short, narrow, and shallow (Figure 2B) while keeping the rest of the channels long, wide, and deep. Away from the T-junction, the inlet channels for both fluids were 300 μm wide and 50 μm deep. At the T-junction, however, the channel carrying the oil phase had a width of 15 μm, depth of 10 μm, and length of 150 μm, while the channel containing the aqueous phase was 7 μm wide, 10 μm deep, and 25 μm long. Downstream from the T-junction, the channel was 1000 μm wide by 50 μm deep, both to minimize the attachment of the droplet to the channel wall and to slow the flow velocity of the droplet.

Figure 2C−F shows the process of encapsulating a single polystyrene bead into the droplet using this method. After the aqueous phase was positioned close to the T-junction, the pressures of both phases were kept constant to maintain the placement of the interface. We then moved our viewing area upstream of the T-junction, after which a single bead was first selected and optically trapped, then optically transported to the T-junction (Figure 2C), and positioned at the interface of the two fluids (Figure 2D). Once the bead was suitably placed, a slightly positive pressure was slowly applied to the aqueous phase so that a single droplet containing the encapsulated bead was sheared off at the interface of the two fluids (Figure 2E,F).

The second method to generate controllably single droplets is to send the aqueous phase through a channel constriction (Figure 2G,H). We based this design on the idea of membrane emulsification, in which one fluid is injected into another immiscible fluid through an orifice or tube.[42,43] By implementing this bulk emulsification strategy in microfluidic systems, we found we can controllably form single droplets on demand. Here we first filled the channel system with the immiscible phase and then introduced aqueous phase into the left reservoir (Figure 2G). Because water does not like the hydrophobic channel walls, the walls were wetted by the immiscible phase. When water was slowly pushed through the orifice, it formed discrete water plugs instead of a continuous stream; these water plugs became droplets after they left the channel constriction and entered the right reservoir that contained the immiscible phase. In this experiment, we used channel constrictions that had a length of 200 μm, width of 15 μm, and depth of 15 μm; the reservoirs and exit had width of 1000 μm and depth of 15 μm. The advantage of this method is that the single droplet can quickly slow as it enters the big oil reservoir and that it is not necessary to flow the immiscible phase at high velocity to shear off aqueous droplets as in the T-channel design. The disadvantage lies in the difficulty with controlling precisely the size of droplets formed.

To selectively encapsulate a bead into the droplet with this method, we first selected, optically trapped and then transported the bead to the interface of the two fluids (Figure 2I,J), followed by application of a slightly positive pressure to the aqueous reservoir, to cause the droplet containing the bead to pinch off (Figure 2K,L). To avoid circulation of the bead at the interface, we continuously trapped and maintained the position of the bead until it was transported away within the droplet during the break off of the droplet.

Stable Encasement of Entrapped Particles in Aqueous Droplets. Once a bead is encased within an aqueous droplet, it is stably confined in the droplet and cannot be removed. Figure 2M−O shows an aqueous droplet (~90 fL) with an entrapped polystyrene bead. The bead could be optically trapped and freely moved inside the water droplet, but it could not be forced across the water/oil interface despite repeated attempts (Figure 2N,O). The polystyrene beads can easily disperse in water because they have negative surface charges due to surface sulfate groups; these negative charges make the dispersion of the beads in the immiscible phase energetically extremely unfavorable. Most biological particles, such as cells, subcellular organelles, and protein complexes, exhibit high surface charges and thus will behave in a manner similar to the bead and be retained stably within the aqueous droplet.

Selective Encapsulation of Single Cells and Subcellular Organelles into Aqueous Droplets. We have successfully encapsulated single cells and single mitochondria that we had selected and optically trapped into individual droplets. Figure 3 shows the encapsulation of a single B lymphocyte (Figure 3A−D) and a single mitochondrion from mast cells (Figure 3E−H) into an aqueous droplet. Similar to the channels in Figure 2A,B,

(39) Courbin, L.; Panizza, P.; Salmon, J. B. *Phys. Rev. Lett.* Art. No. 018305.
(40) Taylor, G. I. *Proc. R. Soc. London, A* **1934**, *146*, 501−523.
(41) Shimada, K.; Kawano, K.; Ishii, J.; Nakamura, T. *J. Food Sci.* **1992**, *57*, 655−656.
(42) Mason, T. G.; Bibette, J. *Langmuir* **1997**, *13*, 4600−4613.
(43) Charcosset, C.; Limayem, I.; Fessi, H. *J. Chem. Technol. Biotechnol.* **2004**, *79*, 209−218.

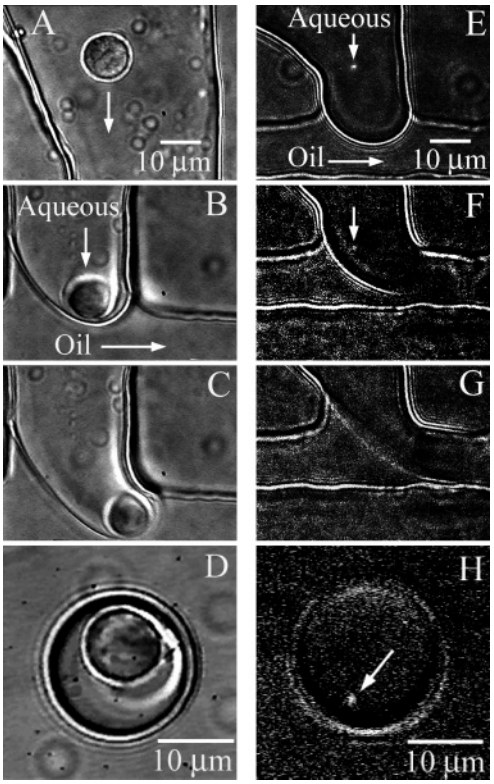

Figure 3. Sequences of images showing the encapsulation of a single B lymphocyte (A−D) and a single mitochondrion (E−H) into an aqueous droplet in silicone oil. Optical trapping was used to transport and position the cell close to the water/oil interface (A−C). An entrapped cell in a droplet is shown in (D). We visualized under fluorescence and optically manipulated a single mitochondrion stained with Mitotracker Green FM at the interface of the two fluids (E, F). Upon application of a pressure pulse to the microchannels (F, G), the mitochondrion was carried away by the flow as the droplet was sheared off. (H) A mitochondrion encapsulated in an aqueous droplet downstream from the T-junction. The scale bar in (A) applies to (B, C) and the one in (E) applies to (F, G).

these channels consisted of two-layer features. The continuous phase we used was silicone oil with 3% (w/w) Span 85.

For the encapsulation of single B lymphocytes (Figure 3A−D), we used culture media with suspended B lymphocytes as our aqueous phase. Similar to the entrapment of a bead, we first selected then optically trapped and transported the single cell to the aqueous/oil interface (Figure 3A,B). We slowly increased the pressure applied to the aqueous phase until the droplet was sheared off at the interface of the two fluids (Figure 3C). Figure 3D shows the encasement of a cell within a droplet.

Figure 3E−H shows the entrapment of a single mitochondrion. Here the mitochondrion was stained with Mitotracker Green FM and suspended in a trypsin−EDTA solution (0.25% trypsin). We used trypsin to minimize the attachment of mitochondria to the PDMS channel walls. Because of the small size of the mitochondrion (<1 μm in diameter), we carried out the encapsulation process under fluorescence (Figure 3E−G). Figure 3H shows a single mitochondrion entrapped in the aqueous droplet that we formed.

The ability to selectively and controllably encapsulate a single cell or subcellular organelle opens new possibilities for carrying out single-cell measurements and single-organelle assays. The volume of the droplet can be made comparable to that of the single cell (Figure 3D) or organelle (Figure 3H), which overcomes challenges associated with diffusion and dilution that would occur if the cell were lysed and chemically manipulated in an open microchannel. The reproducibility and yield of these selective encapsulations of single cells and organelles are very good. In the following, we demonstrate the utility of performing single-cell measurements within aqueous droplets.

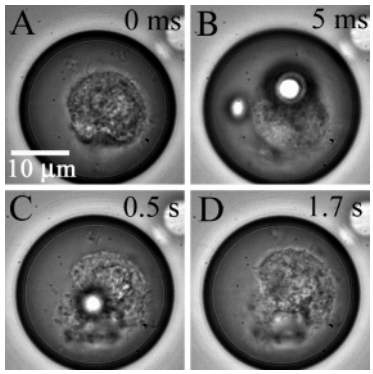

Figure 4. Video sequence acquired by a fast camera that shows the rapid photolysis of a single cell confined within an aqueous droplet in soybean oil. The pulse energy we applied was sufficient to form plasma and cavitation bubbles, which rapidly lyzes the cell (B, C). The scale bar in (A) applies to all panels.

Rapid Photolysis of Single Cells in Aqueous Droplets. Although many chemical and physical manipulations of the encapsulated cell or organelle are possible, such as the chemically induced lysis of the cell and the derivatization of the cellular contents with a fluorophore, we focused on the rapid laser photolysis of the entrapped cell. The attractive aspect of laser photolysis is the rapidity[44−48] by which the cell can be lyzed, so rapid that the cell does not have time to respond and activate its stress signaling pathways.[45] This rapid photolysis, therefore, essentially "freezes" the cellular state at the moment of photolysis and offers a snapshot of the cell's activity at a particular moment in time.

Figure 4 shows the fast photolysis of a single cell in an aqueous droplet surrounded by soybean oil. We used a single ~5-ns pulse from a frequency-tripled YAG (355 nm) to carry out the photolysis. Cell lysis was caused by laser-induced plasma formation and the associated secondary effects (e.g., shock waves and cavitation bubbles).[44,46,47] Although plasma and shock waves form rapidly on the nanosecond scale,[44,46,48] the formation of secondary cavitation bubbles can be observed on the millisecond time scale[44] (see Figure 4B,C).

Unlike cell lysis in bulk liquid, the key advantage in using droplets is the confinement of the single-cell contents within a defined volume. This aspect is particularly important for studying signaling molecules where the copy number present in the cell is low. To facilitate chemical manipulations (e.g., derivatization),

(44) Niemz, M. H. *Laser-Tissue Interactions: Fundamentals and Applications*; Springer-Verlag: Berlin, 2004.
(45) Sims, C. E.; Meredith, G. D.; Krasieva, T. B.; Berns, M. W.; Tromberg, B. J.; Allbritton, N. L. *Anal. Chem.* **1998**, *70*, 4570−4577.
(46) Vogel, A.; Venugopalan, V. *Chem. Rev.* **2003**, *103*, 577−644.
(47) Venugopalan, V.; Guerra, A.; Nahen, K.; Vogel, A. *Phys. Rev. Lett.* Art. No. 078103.
(48) Rau, K. R.; Guerra, A.; Vogel, A.; Venugopalan, V. *Appl. Phys. Lett.* **2004**, *84*, 2940−2942.

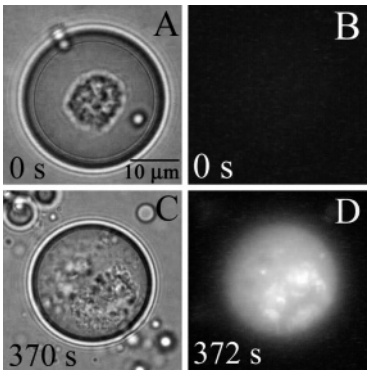

Figure 5. Single-cell enzymatic assay within an aqueous droplet in soybean oil. (A) A mast cell was encapsulated in an aqueous droplet that contained the fluorogenic substrate FDG. (B) Prior to photolysis of the cell, there was little fluorescent product within the droplet because the intracellular enzyme β-galactosidase was physically separated from FDG by the cell membrane. (C, D) After laser-induced cell lysis (C), β-galactosidase catalyzed the formation of the product fluorescein, which caused the droplet to become highly fluorescent (D). The scale bar in (A) applies to all panels.

the concentration of the single-cell contents can be further concentrated.[2] Because of the slow dissolution of the water molecules (e.g., minutes for soybean oil[2]) from the aqueous droplet into the immiscible phase, the concentration of the entrapped solute (e.g., amino acids, proteins, and DNA) can be increased by many orders of magnitude.[2] In addition, individual droplets can be physically manipulated,[1,20] transported,[20] and fused,[1] thereby offering an attractive platform for carrying out single-cell studies.

Single-Cell Assays in Aqueous Droplets. We used individual droplets as picoliter- and femtoliter-sized bioreactors to assay the enzymatic activity of a single cell. Here the aqueous solution of the droplet contained a fluorogenic substrate, FDG, for intracellular β-galactosidase. The substrate and enzyme were physically separated from each other by the cell membrane. Upon photolysis of the cell, however, the cell membrane was compromised so the enzymatic reaction was permitted to take place. Prior to photolysis (Figure 5A,B), the fluorescence background was low. Several minutes after photolysis (Figure 5C,D) the droplet became highly fluorescent, owing to the formation of the fluorescent product (fluorescein) from the enzymatic reaction. This single-cell enzymatic assay was very reproducible. Here the droplet confines the lysate and fluorescent product within a small finite volume. Without this confinement, both the enzyme and fluorescein would diffuse and would be rapidly diluted to a large area, which would make the accumulation of the fluorescent product difficult to follow. There were localized bright areas within the droplet because of the association of the enzyme and product with the intracellular membrane compartments.

CONCLUSION

Because of the confined finite volumes in pico- and femtoliter-volume droplets and because in principle large numbers of droplets containing different aqueous solutions can be generated and manipulated in parallel, we believe such droplets offer an attractive format for carrying out single-cell and single-organelle studies. Here we demonstrated the first steps toward this goal, namely, the ability to generate a single droplet on demand and to entrap a selected target cell or organelle into the droplet, followed by simple in-droplet manipulation (laser-induced lysis) and enzymatic assay. In these examples, spatial confinement within the droplet prevented rapid dilution of the cellular contents after lysis and during enzymatic assay. With further development, the droplet manipulations we demonstrated here can be combined with droplet fusion for initiating chemical reactions, such as derivatization, and capillary electrophoresis separation for carrying out more sophisticated chemical analysis and biological studies on single cells and subcellular organelles.

ACKNOWLEDGMENT

R.M.L. thanks the Center for Nanotechnology at the UW for an NSF-supported IGERT Fellowship Award (DGE-9987620). We gratefully acknowledge support of this work from the National Institute of Health (GM65293-01) and the Keck Foundation.

Received for review December 27, 2004. Accepted January 17, 2005.

AC0480850